Research Article

Chlorpromazine and Promethazine (C+P) Reduce Brain Injury after Ischemic Stroke through the PKC-δ/NOX/MnSOD Pathway

Sichao Guo ⬚,[1,2,3] Fengwu Li ⬚,[1] Melissa Wills,[2] James Yip ⬚,[2] Alexandra Wehbe ⬚,[2,4] Changya Peng,[2,3] Xiaokun Geng ⬚,[1,2,5] and Yuchuan Ding ⬚[2,3]

[1]*Luhe Institute of Neuroscience, Beijing Luhe Hospital, Capital Medical University, Beijing 101100, China*
[2]*Department of Neurosurgery, Wayne State University School of Medicine, Detroit, MI 48201, USA*
[3]*Department of Research & Development Center, John D. Dingell VA Medical Center, Detroit, MI 48201, USA*
[4]*Harvard T.H. Chan School of Public Health, Boston, MA 02115, USA*
[5]*Department of Neurology, Beijing Luhe Hospital, Capital Medical University, Beijing 101100, China*

Correspondence should be addressed to Xiaokun Geng; xgeng@ccmu.edu.cn and Yuchuan Ding; yding@med.wayne.edu

Cerebral ischemia-reperfusion (I/R) incites neurologic damage through a myriad of complex pathophysiological mechanisms, most notably, inflammation and oxidative stress. In I/R injury, nicotinamide adenine dinucleotide phosphate (NADPH) oxidase (NOX) produces reactive oxygen species (ROS), which promote inflammatory and apoptotic pathways, augmenting ROS production and promoting cell death. Inhibiting ischemia-induced oxidative stress would be beneficial for reducing neuroinflammation and promoting neuronal cell survival. Studies have demonstrated that chlorpromazine and promethazine (C+P) induce neuroprotection. This study investigated how C+P minimizes oxidative stress triggered by ischemic injury. Adult male Sprague-Dawley rats were subject to middle cerebral artery occlusion (MCAO) and subsequent reperfusion. 8 mg/kg of C +P was injected into the rats when reperfusion was initiated. Neurologic damage was evaluated using infarct volumes, neurological deficit scoring, and TUNEL assays. NOX enzymatic activity, ROS production, protein expression of NOX subunits, manganese superoxide dismutase (MnSOD), and phosphorylation of PKC-δ were assessed. Neural SHSY5Y cells underwent oxygen-glucose deprivation (OGD) and subsequent reoxygenation and C+P treatment. We also evaluated ROS levels and NOX protein subunit expression, MnSOD, and p-PKC-δ/PKC-δ. Additionally, we measured PKC-δ membrane translocation and the level of interaction between NOX subunit (p47^{phox}) and PKC-δ via coimmunoprecipitation. As hypothesized, treatment with C+P therapy decreased levels of neurologic damage. ROS production, NOX subunit expression, NOX activity, and p-PKC-δ/PKC-δ were all significantly decreased in subjects treated with C+P. C+P decreased membrane translocation of PKC-δ and lowered the level of interaction between p47^{phox} and PKC-δ. This study suggests that C+P induces neuroprotective effects in ischemic stroke through inhibiting oxidative stress. Our findings also indicate that PKC-δ, NOX, and MnSOD are vital regulators of oxidative processes, suggesting that C+P may serve as an antioxidant.

1. Introduction

Acute ischemic stroke results in permanent neurologic damage, contributing to its high morbidity and mortality rates internationally and high health care costs annually [1]. Reperfusion strategies, such as tissue plasminogen activator (tPA) and thrombectomy, are the standard for treating acute ischemic stroke and have been the primary focus of technological advances in stroke therapy [2]. However, even in the event of successful recanalization, morbidity rates remain high and clinical outcomes are often poor due to complicating reperfusion injury [3, 4]. It is imperative to explore other therapeutic methods, such as neuroprotective and neuro-rehabilitative strategies, to maximize functional outcomes and patient quality of life.

Chlorpromazine and promethazine (C+P), two pheno-thiazine drugs, are commonly utilized for their sedative and antipsychotic effects [5]. C+P induces a state of "arti-ficial hibernation," an effect found to confer neuroprotection in cerebral ischemia [5–7]. Previous studies suggest that the hypothermia induced by this state of hibernation is key to its potent neuroprotective properties. Reduced body tem-peratures and metabolic rates confer a higher tolerance to ischemia, hypoglycemia, and other conditions of low perfu-sion states, thus presenting more favorable parameters for patients with acute ischemic stroke. Pharmacological hypo-thermia, induced by drugs such as C+P, evades many poten-tial complications associated with therapeutic hypothermia induced through external or endovascular cooling methods, such as coagulopathy, hypokalemia, and infection [8]. How-ever, some studies have shown that the neuroprotective mechanisms of C+P are independent or only partially dependent on temperature, thus suggesting that C+P's neu-roprotective effects may be due to a separate, temperature-independent mechanism [5, 9]. Phenothiazines have been found to protect the in vitro human neuroblastoma cell line SHSY5Y from oxidative stress triggered by both exogenic and mitochondrial free radicals. Phenothiazines act as neu-roprotectants by both scavenging free radicals and inducing antioxidant protein synthesis [10]. Furthermore, prometha-zine was shown to be protective in stroke models by target-ing the mitochondrial permeability transmission (mPT), which, when activated, has been linked to cytotoxicity after infective, ischemic, and excitotoxic pathological insults [11].

Dual therapy with C+P has been found to have a signif-icant protective effect on neurologic tissue in both transient and permanent ischemic strokes. C+P has been found to decrease infarction volumes, improve long-term motor per-formance, and minimize metabolic damage [5]. Prior studies have suggested that C+P may induce neuroprotection through changes in protein levels of PKC-δ and nicotin-amide adenine dinucleotide phosphate oxidase (NOX) [5, 12], which are protein complexes heavily involved in oxidative stress and cell destruction after ischemic stroke. However, the specific mechanism by which C+P inhibits oxidative stress through the PKC-δ/NOX pathway is still unclear. To fully understand the neuroprotective effects of C+P, this study investigated mechanisms by which C+P inhibits oxidative stress after stroke.

Excess oxygen and reactive oxygen species (ROS) are widely known to produce oxidative stress, causing cellular damage after ischemic stroke [13]. NOX, a multi-subunit enzyme, employs nicotinamide adenine dinucleotide phos-phate (NADP+) to generate ROS and superoxide anions [14]. Increases in NOX activity, NOX subunit expression, and cell death have been found after ischemia/reperfusion (I/R) and are associated with larger infarct volumes and worse functional outcomes [14–16]. NADPH oxidase is comprised mainly of p22$^{\text{phox}}$ (phox, phagocyte oxidase), p47$^{\text{phox}}$, and p67$^{\text{phox}}$, which are regulatory subunits, and cat-alytic subunit gp91$^{\text{phox}}$ [17]. The brain has been previously shown to express the major NOX subunits (p22$^{\text{phox}}$, p47$^{\text{phox}}$, p67$^{\text{phox}}$, and gp91$^{\text{phox}}$) [15] and activate NOX, which aggra-vates I/R injury by overproducing ROS [15]. Additionally,

protein kinase C (PKC) acts as a key activator of NADPH oxidase [18]. As a member of the PKC family, PKC-δ acti-vates NOX during I/R, augmenting oxidative damage and cell apoptosis [12]. Conversely, manganese-containing superoxide dismutase (MnSOD), a vital antioxidant enzyme in the central nervous system, is a main pathway through which cells resist ROS damage after cerebral ischemia [19].

Our study sought to delineate the antioxidation mecha-nism by which C+P induces neuroprotective effects by asses-sing the PKC-δ/NOX/MnSOD pathway, as well as the capacity of these drugs to repair oxidative damage after ischemic stroke. A robust understanding of the oxidative pathway of neuroprotection after ischemic stroke would guide future endeavors in finding therapeutic targets that capitalize on these processes to improve patient morbidity and mortality.

2. Materials and Methods

2.1. Subjects. 142 adult male Sprague-Dawley rats (280–300 g, Beijing Vital River Laboratory Animal Technology Company, Limited) served as the subjects of our study. We followed the Institutional Animal Investigation Committee of the Capital Medical University standard operating proce-dures (89E58F61-7D97-4FA1-B7D0-02DA47F7A735). The animals were caged and subjected to a 12-hour light/dark cycle for the duration of the experiment. All possible steps were taken to minimize harm to the rats and the quantity of rats used. The rats were separated into six groups ran-domly: (1) a sham group that did not undergo middle cere-bral artery occlusion (MCAO) ($n = 12$); (2) two-hour MCAO before reperfusion for 6 or 24 hours ($n = 26$); (3) two-hour MCAO and C+P with temperature control at 37°C before reperfusion for 6 or 24 hours ($n = 26$); (4) two-hour MCAO and C+P without temperature control before reperfusion for 6 or 24 hours ($n = 26$); (5) two-hour MCAO and NOX inhibitor before reperfusion for 6 or 24 hours ($n = 21$); and (6) two-hour MCAO and PKC-δ inhibitor before reperfusion for 6 or 24 hours ($n = 21$). Ten rats (<10%) were not included in further analysis due to either cerebral hemorrhage, death, or absence of ischemic injury based on neurological deficit scoring and TTC staining. The experiment and statistical analysis were conducted in a random and blinded fashion [20]. For the temperature-controlled groups, rats were put under warm ambient light on 37°C insulation blankets to maintain body temperature. For the non-temperature-controlled groups, animals were stored in a 25°C facility. Due to the intimate linkage between cerebral and body temperatures [21], rectal temperatures were monitored to lower the risk of intracranial hemorrhage.

2.2. Focal Cerebral Ischemia. We have previously explained the model of regional cerebral ischemia employed for this study [22]. In summary, the subjects were placed within a chamber and anesthetized with 1–3% isoflurane and a 30% oxygen and 70% nitrous oxide solution. Using a face mask, anesthesia was with 1% isoflurane administered via a cali-brated precision vaporizer. To minimize variability between rodents and yield consistently sized infarcts, the MCA was

occluded using 4.0 poly-L-lysine-coated intraluminal nylon sutures for each procedure.

2.3. Chlorpromazine+Promethazine Administration and NOX Inhibitor/PKC-δ Inhibitor.

In equal parts, rats received 8 mg/kg of C+P intraperitoneally (IP) when reperfusion began, the parameters of which were validated in a prior study [5]. One to two hours later, rats were given another injection, which was dosed at one-third of the original dose of C+P, to augment the C+P's therapeutic effects. Either a NOX inhibitor, apocynin (2.5 mg/kg), or a PKC-δ inhibitor, rottlerin (0.3 mg/kg), was injected IP 2 hours from initiation of MCAO.

2.4. Cell Culture and Oxygen Glucose Deprivation/Reoxygenation (OGD/R) with C+P Administration.

The cell line of human SHSY5Y was acquired from ATCC. We incubated cells in a $25 cm^2$ culture flask with 5 ml of DMEM/F12 and 10% FBS and cultured to nine to eleven passages. We incubated the cells at 5% CO_2 and 37°C in a humidified incubator, explained in a previous study by us [23].

To execute the OGD model, described in a previous study by us, an anaerobic chamber flushed with 95% N_2 and 5% CO_2 (v/v) maintained at 37°C was used [23]. We replaced culture medium with deoxygenated and glucose-free DMEM to begin two hours of OGD. The SHSY5Y cells were taken out of the anaerobic chamber, and the DMEM medium was exchanged with maintenance medium, with subsequent C+P treatment. C+P had a final concentration of 2.5 μM, determined in a prior project conducted by us. Lastly, in a humidified incubator, cells were cultured for either 6 or 24 hours before harvest.

2.5. Infarct Volume Measurement.

After being removed from the cranial cavity, the brain matrix was cut into 2 mm thick slices and stained using 2,3,5-triphenyltetrazolium chloride after reperfusion for 48 hours. Infarction volumes were calculated indirectly to minimalize error caused by edema. Cross-sectional areas of the infarcted regions in each slice were computed with ImageJ. Infarction volume for each slice was computed as the difference between total left hemisphere volume and volume of the noninfarcted right hemisphere, then divided by the total volume of the left hemisphere [24].

2.6. TUNEL Assay.

The TUNEL assay was employed for evaluating DNA fragmentation using a commercial kit as outlined in prior work conducted by us [24, 25]. Images were obtained randomly from territory supplied by the MCA. Complying with the manufacturer's indications, the permeabilized and fixed slides were incubated in 50 μl of TUNEL reaction mixture for one hour at 37°C. Positive TUNEL staining was visualized with fluorescent microscopy. The TUNEL^{+} cells were counted using the ImageJ manual cell counting tool. The cell counts from every section from each group for the statistical analysis were blindly obtained. The total cell number was acquired via counting the DAPI^{+} cells, including each dead cell. From each rat, a slide was selected ($n = 5$), and four regions of interest were assessed from each slide. The percent of apoptotic cells was computed and averaged as the (total TUNEL^{+} cells in all 20 regions/total cells in all 20 regions) × 100%. Because the images were acquired randomly from four separate areas in MCA-supplied territory, findings signify cell death of the area of ischemia.

2.7. Cell Death Detection.

Apoptotic cell death was assessed by a photometric enzyme immunoassay explained in a previous study conducted by us [26]. The number of cytoplasmic histone-associated DNA fragments created through apoptotic cell death was assessed. Subsequently, light absorbance at a 405 nm wavelength was computed.

2.8. NADPH Oxidase Activity.

Right cerebral hemisphere sample tissues were processed using methods explained in our prior study [27]. In summary, cerebral tissue samples were homogenized with lysis buffer. In each well of the luminescence plate, 80 μl lucigenin mix and 20 μl of homogenate were added and subsequently incubated at 37°C for 10 minutes. The final concentration of NADPH, 0.1 mM, was then added, and we determined luminescence using the DTX-880 multimode detector for thirty seconds per specimen, totaling at ten minutes.

2.9. ROS Assay.

Neurologic tissue samples comprised of MCA-supplied territories, the frontoparietal cortex, and striatum were analyzed. The Amplex Red Hydrogen Peroxide/Peroxidase Assay Kit was used to identify ROS, which we described in a prior study [28]. In the brain homogenates, the amount of H_2O_2 was measured with a DTX-880 Multimode Detector.

To measure ROS production in cells, we utilized DCFH-DA (2,7-dichlorodihydrofluorescein diacetate), which we explained in a prior study [23]. Cultures were washed one time using PBS and then stained with 25 μM DCFDA in 100 μl PBS at 37°C for a half hour. Cultures were washed thrice with PBS prior to signal reading at Ex/Em 485/535 nm.

2.10. Coimmunoprecipitation (Co-IP).

Coimmunoprecipitation of PKC-δ with p47[phox] was performed. Cell supernatants were collected 6 and 24 hours after OGD/R. Cell lysis buffer (9803, CST) was used to collect the lysates. For 15 minutes and at 4°C, the lysates were centrifuged at 13,000 rpm prior to collecting the supernatants. Primary anti-PKC-δ (sc-213, Santa Cruz Biotechnology) and anti-IgG antibody (2729, Cell Signaling Technology) were added to 200 μl cell lysate and incubated at 4°C overnight. Antibody immunocomplex solution and lysate were transferred to the protein G magnetic bead-containing tube and incubated with rotation at room temperature for 20 minutes. Magnetic Separation Rack (7017, Cell Signaling Technology) was used to separate the magnetic beads in accordance with the manufacturing directions and then boiled to denature the protein-bead complex. The immunoprecipitants from cells underwent Western blot analysis. Primary anti-PKC-δ (9616, Cell Signaling Technology) and anti-p47[phox] (4312, Cell Signaling Technology) were used for Western blot detection.

2.11. Cellular Subfraction Analysis. The subcellular protein fractionation kit for cultured cells was used to execute the subcellular fractionation in accordance with manufacturing directions [29]. Whole cell lysates which were cultured to confluence were prepared using lysis buffer that included protease inhibitors. Proteins were then separated by SDS PAGE. The primary antibodies used were anti-PKC-δ and Na$^+$/K$^+$ ATPase as indicators of membrane subfraction, whereas α-tubulin was used as the indicator for the cytoplasm subfraction.

2.12. Protein Expression. Protein expression in brain tissue and cells was detected using Western blot analysis, which we have described in a prior study [28]. The frontoparietal cortex and striatum (right cerebral hemisphere components) were managed as the tissue sample for subsequent evaluation. A mammalian protein extraction reagent was used to lyse tissues and cells. Isolated rodent brain protein and cell isolates were then loaded onto electrophoresis gels. Then, proteins were moved to a polyvinylidene fluoride membrane. Membranes were then incubated with primary antibodies (1 : 1,000, rabbit anti-PKC-δ antibody; 1 : 1,000, anti-p-PKC-δ antibody; 1 : 1,000, rabbit anti-p47^{phox}; 1 : 1,000, rabbit anti-p22^{phox}; 1 : 1,000, rabbit anti-gp91^{phox}; 1 : 1,000, rabbit anti-p67^{phox}; 1 : 1,000, anti-MnSOD antibody; and 1 : 2,000, β-actin) for 16 hours at 4°C. Subsequently, membranes were then incubated using a secondary antibody (goat anti-rabbit IgG) for 2 hours at room temperature. Immunoreactive bands were identified with an enhanced chemiluminescence system. For each antibody, Western blot images were studied with ImageJ to quantify relative image density of protein expression.

2.13. Statistical Analysis. GraphPad Prism v8.0 (San Diego, California, United States) was used to conduct the statistical analyses. Using one-way ANOVA, differences among groups were computed with a predetermined significance level of $p < 0.05$. Post hoc comparison among groups was done using the least significant difference (LSD) method. Data are presented as the mean ± SE.

3. Results

3.1. C+P Minimized Neurologic Injury Postischemia-Reperfusion. Body temperature was significantly reduced as early as 5 minutes post-C+P treatment for the non-temperature-controlled C+P group versus the I/R or C+P at 37°C groups. Around 2 hours posttreatment, body temperatures were lowered to 34°C. Body temperatures continued to be significantly lowered for up to 6 hours, prior to spontaneously returning to normothermic levels (Figure 1(a)).

In comparison to the ischemic group with the greatest cerebral infarction volume at 48 hours of reperfusion (Figure 1(b)), infarct volumes were significantly reduced for both temperature-controlled and non-temperature-controlled C+P groups. Neurologic deficits were determined by previously validated 5- or 12-point scoring systems at 48 hours of reperfusion (Figure 1(c)). Compared with the

I/R group, C+P administration in the non-temperature-controlled groups inhibited 5-point scoring system scores, indicating lower levels of neurological damage ($p < 0.05$). Similarly, the non-temperature-controlled C+P and C+P temperature-controlled groups ($p < 0.05$, $p < 0.001$) had lower 12-point scoring system scores, also indicating reduced neurologic damage. To examine the fundamental physiology behind C+P's neuroprotective effects in the context of the PKC-δ/NOX pathway post-stroke, we gave PKC-δ and NOX inhibitors. NOX and PKC-δ inhibition significantly reduced infarct volumes and neurological deficits at 48 hours of reperfusion (Figures 1(b) and 1(c)).

Apoptotic cell death assessed using ELISA was amplified post-MCAO as compared to the sham group but decreased after C+P administration at 6 and 24 hours after reperfusion ($p < 0.05$, $p < 0.01$) (Figure 1(d)). Additionally, the NOX and PKC-δ inhibitors significantly attenuated the higher levels of cell apoptosis, except for NOX inhibition groups after 6 hours of reperfusion (Figure 1(d)). Moreover, apoptotic cell death determined by the TUNEL assay was significantly reduced in groups who received C+P regardless of temperature control status ($p < 0.001$) (Figure 1(e)).

3.2. C+P Treatment Attenuated ROS Levels and NOX Activity Postreperfusion. In rats subject to 2 hours of MCAO, cerebral NOX activity was significantly higher at 24 hours of reperfusion. Adding C+P reduced NOX activity ($p < 0.001$). Moreover, NOX and PKC-δ inhibitors significantly lowered NOX activity at 24 hours of reperfusion (Figure 2(a)). We also found a significant surge in ROS generation at both 6 and 24 hours of reperfusion in neurologic tissue; however, C+P administration significantly reduced these ROS levels (Figure 2(b)). The NOX and PKC-δ inhibitors also reduced ROS at 6 and 24 hours of reperfusion ($p < 0.001$) (Figure 2(b)). Additionally, we examined C+P's influence on SHSY5Y cells with OGD/R. While ROS levels were raised at 6 and 24 hours of reoxygenation, C+P administration offered ($p < 0.05$) significant protection to the cells by inhibiting ROS production (Figure 2(c)).

3.3. C+P Treatment Decreased NOX Subunit Expression. The ischemic group demonstrated significant enhancement of NOX subunit expression (gp91^{phox}, p67^{phox}, p47^{phox}, and p22^{phox}) at 24 hours of reperfusion ($p < 0.01$, $p < 0.001$). Both C+P therapy groups demonstrated decreased NOX subunit levels at 24 hours of reperfusion except p22^{phox} in the temperature-controlled C+P group (Figures 3(a)–3(d)). There was a larger decrease in p22^{phox} expression for non-temperature-controlled groups compared to temperature-controlled groups administered with C+P at 24 hours of reperfusion ($p < 0.001$) (Figure 3(d)). Also, NOX and PKC-δ inhibitors significantly reversed the raised NOX subunit levels at 24 hours of reperfusion ($p < 0.01$, $p < 0.001$) (Figures 3(a)–3(d)).

Also, in SHSY5Y cells with OGD/R treatment, levels of gp91^{phox} and p67^{phox} were enhanced at 24 hours of reoxygenation when assessed against the control group ($p < 0.05$); however, C+P significantly annulled raised gp91^{phox} and p67^{phox} protein levels (Figures 4(a) and 4(b)). OGD
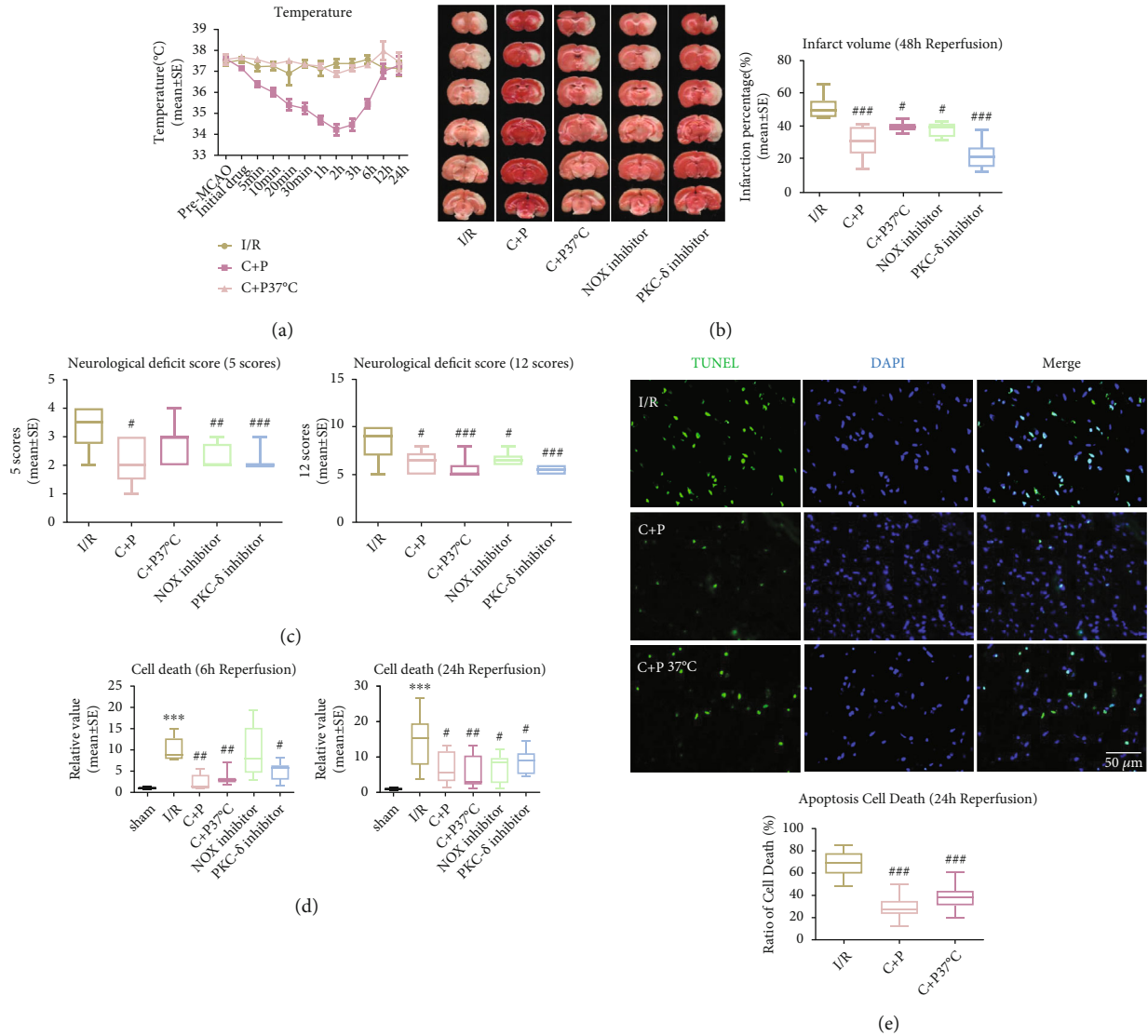
(a)

(b)

(c)

(d)

(e)

FIGURE 1: C+P lessened postischemic neurologic damage. (a) Alterations in body temperature post C+P administration at various points in time in 2-hour MCAO and after reperfusion (0–24 hours). Baseline temperatures were determined just before MCAO. Reperfusion was followed by C+P administration. ANOVA analyses specified that C+P significantly decreased body temperatures as early as 5 minutes and lasting up to 6 hours after the I/R onset ($n = 7$). (b) TTC stains showcase infarction volumes in MCAO rats regardless of C+P treatment at 48 hours of reperfusion. C+P administration or administration of the PKC-δ/NOX inhibitor significantly decreased infarct volumes ($n = 7$). (c) Neurologic deficits were determined using 5- or 12-point scoring systems at 48 hours of reperfusion. C+P administration or the administration of the PKC-δ/NOX inhibitor significantly reduced neurological deficits in all groups except those in the temperature-controlled C+P group, for which there was no effect on the 5-point scoring system ($n = 7$). (d) Cell death was significantly higher at 6 and 24 hours of reperfusion, demonstrated by ELISA. With C+P at 6 and 24 hours of reperfusion, cell death was significantly reduced. Administration of the PKC-δ/NOX inhibitor also suppressed cell death except in the NOX inhibitor group at 6 hours of reperfusion ($n = 7$). (e) Apoptotic cell death was significantly reduced with C+P administration regardless of temperature control at 24 hours of reperfusion, shown using the TUNEL assay ($n = 5$). Scale bar = 50 μm. ***$p < 0.001$ versus the sham group; #$p < 0.05$, ##$p < 0.01$, and ###$p < 0.001$ versus the I/R group. Results are shown as mean ± SE.

enhanced levels of p47^{phox} at 6 and 24 hours of reoxygenation ($p < 0.05$). Furthermore, C+P administration also lowered levels of p47^{phox} protein levels ($p < 0.05$, $p < 0.01$) at 6 and 24 hours of reoxygenation (Figure 4(c)). At 6 hours of reoxygenation, OGD-induced upregulation of p22^{phox} ($p < 0.05$) was negated by C+P treatment ($p < 0.01$) (Figure 4(d)).

3.4. C+P Treatment Suppressed Phosphorylation PKC-δ Activation.
Since PKC-δ phosphorylation influences its catalytic activity [30], we investigated levels of both total and phosphorylated PKC-δ. In brain tissue, p-PKC-δ concentration was raised at 6 hours of reperfusion ($p < 0.01$). C+P treatment resulted in significantly lowered p-PKC-δ compared with I/R groups. Total PKC-δ levels increased in the
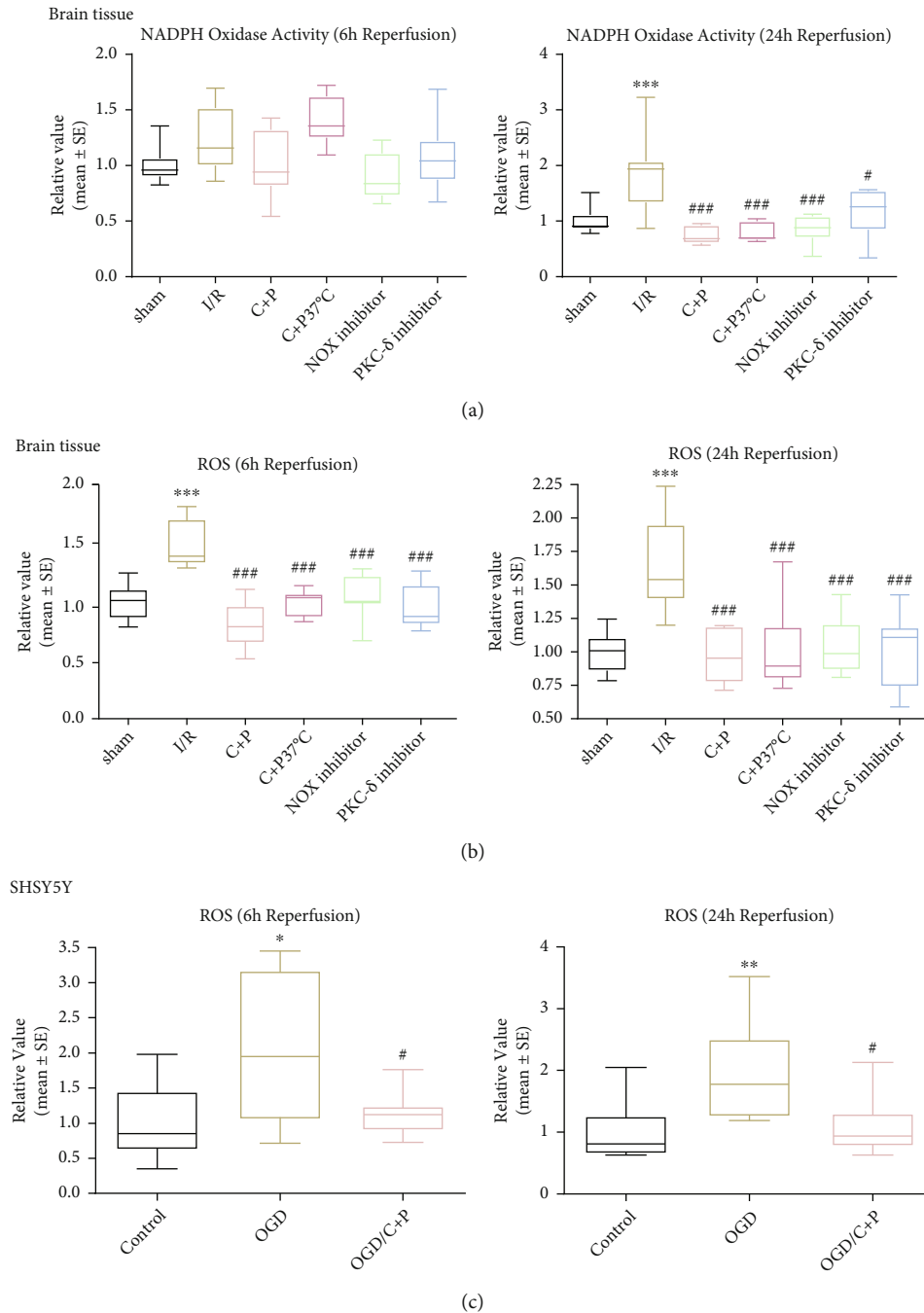
(a)

(b)

(c)

Figure 2: C+P attenuated NOX activity and ROS level postreperfusion. Quantitative analysis of (a) NOX activity and (b) ROS level as determined in ischemic brain tissue. NOX activity was higher at 24 hours of reperfusion, and ROS levels were also higher at 6 and 24 hours of reperfusion. Decreased NOX activity levels at 24 hours of reperfusion and ROS at 6 and 24 hours of reperfusion were observed in C+P groups regardless of temperature control as well as in PKC-δ or NOX inhibitor groups ($n = 7$). $^{***}p < 0.001$ versus the sham group; $^{#}p < 0.05$, $^{###}p < 0.001$ versus the I/R group. Data is shown as the mean ± SE. Quantitative analysis of (c) ROS level in SHSY5Y cell was measured. C+P administration lowered the OGD-induced elevation of ROS at 6 and 24 hours of reoxygenation. $^{*}p < 0.05$, $^{**}p < 0.01$ versus the OGD group; $^{#}p < 0.05$ versus the OGD/C+P group. Results are shown as mean ± SE of three independent experiments.

infarcted area at 24 hours of reperfusion ($p < 0.05$). C+P decreased total PKC-δ protein levels ($p < 0.05$, $p < 0.001$). Additionally, the p-PKC-δ/PKC-δ ratio significantly increased post-MCAO ($p < 0.01$); however, the ratio decreased when C+P was administered at 6 hours of reperfusion ($p < 0.001$) (Figure 5(a)). In SHSY5Y cells at 24 hours of

reoxygenation, both p-PKC-δ and PKC-δ levels were elevated after OGD ($p < 0.05$) whereas C+P administration reduced these levels ($p < 0.05$). Also, the p-PKC-δ/PKC-δ ratio rose post-OGD/R ($p < 0.05$, $p < 0.001$) but was suppressed by C+P treatment at 6 and 24 hours of reoxygenation ($p < 0.05$, $p < 0.001$) (Figure 5(b)).
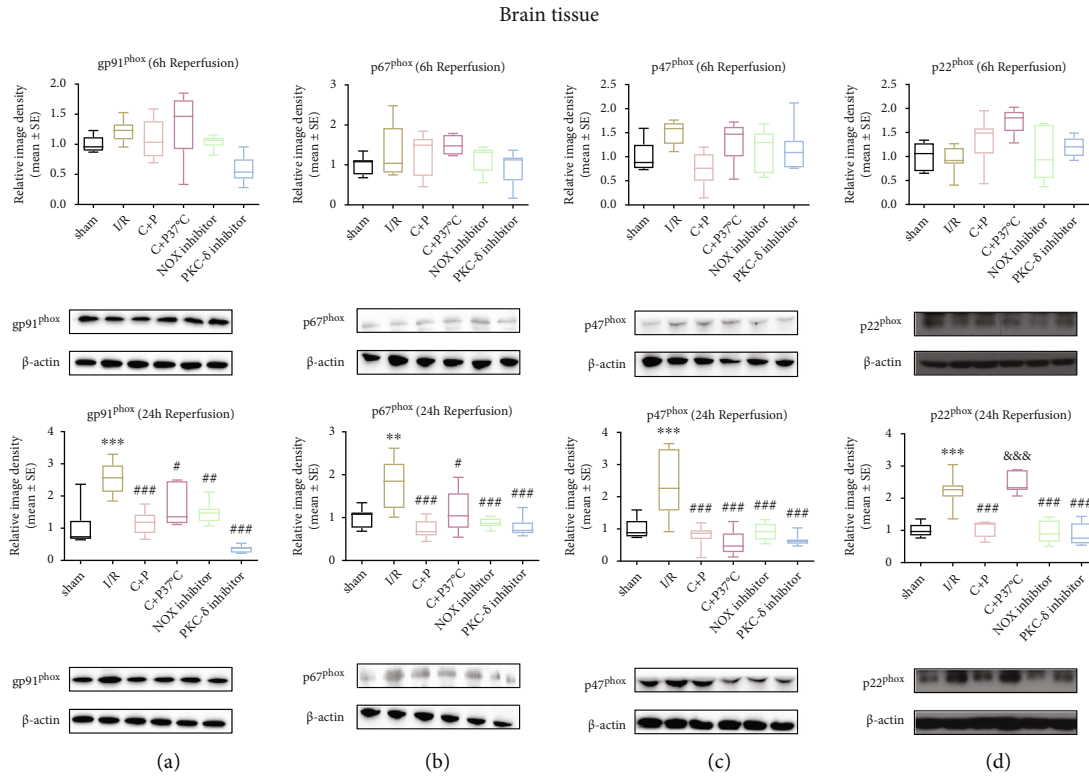
Brain tissue

Figure 3: C+P decreased NOX subunit protein levels after stroke in ischemic brain tissue. (a) gp91^{phox}, (b) p67^{phox}, (c) p47^{phox}, and (d) p22^{phox} assessed via the Western blot technique at 6 and 24 hours of reperfusion. Levels of gp91^{phox}, p67^{phox}, p47^{phox}, and p22^{phox} rose after I/R but decreased after C+P treatment and administration of the PKC-δ or NOX inhibitor at 24 hours of reperfusion, with the exception of p22^{phox} in the C+P at the 37°C group at 24 hours of reperfusion. There was a larger decrease in p22^{phox} expression in the non-temperature-controlled C+P versus the temperature-controlled C+P group at 24 hours of reperfusion ($n = 7$). $^{**}p < 0.01$ and $^{***}p < 0.001$ versus the sham group; $^{\#}p < 0.05$, $^{\#\#}p < 0.01$, and $^{\#\#\#}p < 0.001$ versus the I/R group; $^{\&\&\&}p < 0.001$ versus the C+P group. Results are shown as mean ± SE. The representative immunoblots are visualized.

3.5. C+P Treatment Decreased PKC-δ Translocation.

Western blot analyses were performed to investigate PKC-δ cytosolic and membrane expression of SHSY5Y cells, presented in Figure 6(a). In comparison to the control group, cytosolic expression of PKC-δ expression decreased ($p < 0.05$) and membrane expression increased ($p < 0.05$) in the OGD/R group at 6 hours after reoxygenation, whereas C+P treatment prevented changes in PKC-δ expression caused by OGD/R ($p < 0.05$, $p < 0.01$). Against the OGD/R group at 24 hours of reoxygenation to the control, no differences in PKC-δ expression in the cytosol were seen; however, there was significantly increased PKC-δ expression in the membrane ($p < 0.05$). C+P lessened increased membrane PKC-δ expression ($p < 0.05$).

3.6. C+P Treatment Inhibited PKC-δ and p47^{phox} Interaction.

In order to determine the functional interaction of PKC-δ and p47^{phox}, whole cell lysates from neuronal SHSYSY cells were immunoprecipitated with PKC-δ or IgG antibody followed by antibody treatment against PKC-δ and p47^{phox} with Western blot. The IgG antibody served as the control. In comparison to the IgG control, significant increases in p47^{phox} were detected in the immunoprecipitation complex with the PKC-δ antibody from cell lysates, indicating an interaction between PKC-δ and p47^{phox}.

Moreover, after 6 hours of reoxygenation, OGD resulted in increased interaction of PKC-δ and p47^{phox} ($p < 0.05$), whereas treatment with C+P reduced interaction ($p < 0.05$). There was also an observable, but statistically insignificant increase in the interaction between the control and OGD groups at 24 hours of reoxygenation while C+P treatment attenuated the interaction of PKC-δ and p47^{phox} ($p < 0.01$) (Figure 6(b)).

3.7. C+P Promoted Increased Expression of MnSOD.

MnSOD levels were significantly decreased for the 2-hour MCAO/24-hour reperfusion group ($p < 0.05$). However, treatment with C+P significantly reversed these decreased MnSOD levels, regardless of temperature control ($p < 0.001$) (Figure 7(a)). Similarly, in the cell experiments, OGD induced a significant reduction of the MnSOD level at 24 hours of reoxygenation. As hypothesized, C+P administration significantly increased MnSOD expression at both 6 and 24 hours of reoxygenation ($p < 0.05$) (Figure 7(b)).

4. Discussion

This study sought to explore C+P-induced neuroprotection after ischemic stroke. Our findings reinforce findings from previous studies which assert that treatment with C+P
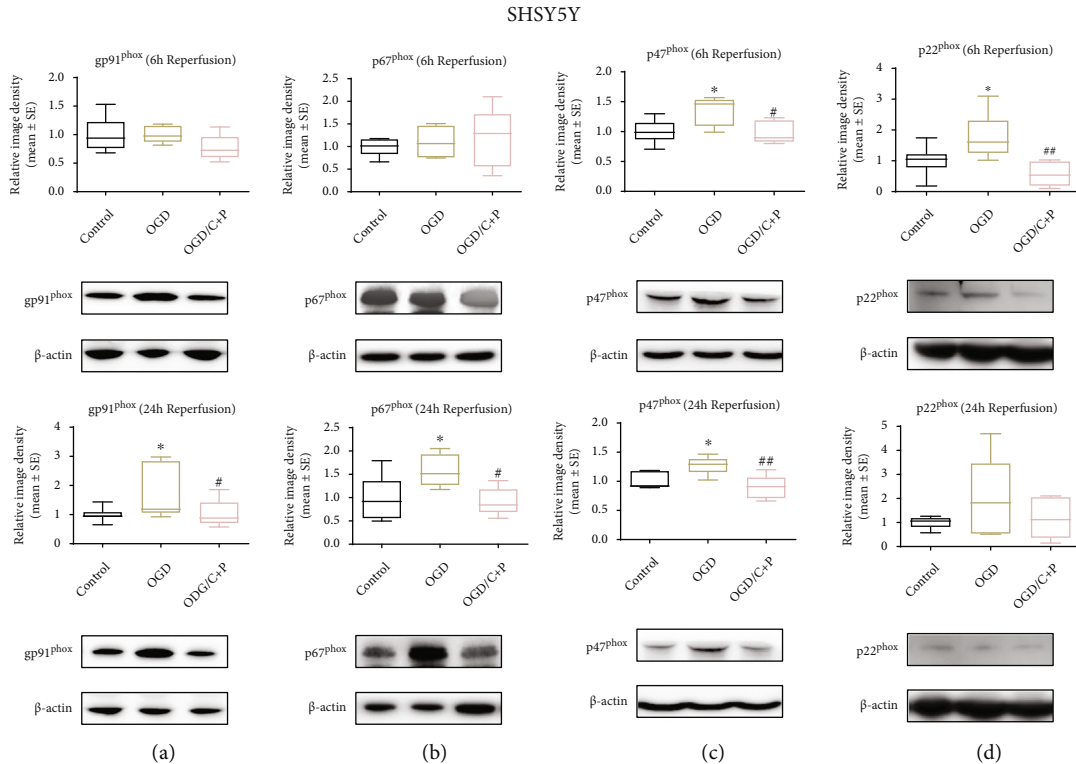
SHSY5Y

(a)   (b)   (c)   (d)

Figure 4: C+P reduced protein levels of NOX subunits after OGD/R in SHSY5Y cells. (a) gp91$^{\text{phox}}$, (b) p67$^{\text{phox}}$, (c) p47$^{\text{phox}}$, and (d) p22$^{\text{phox}}$, identified by Western blot at 6 and 24 hours of reoxygenation. Levels of gp91$^{\text{phox}}$ and p67$^{\text{phox}}$ protein increased after OGD but decreased after C+P therapy at 24 hours of reoxygenation. Moreover, p47$^{\text{phox}}$ levels increased after OGD, but C+P lowered this expression at 6 and 24 hours of reoxygenation. OGD induced the elevation of p22$^{\text{phox}}$, and there was a greater reduction in p22$^{\text{phox}}$ expression in the OGD/C+P treatment group versus the OGD group at 6 hours of reoxygenation. $^{*}p < 0.05$ versus the OGD group; $^{\#}p < 0.05$, $^{\#\#}p < 0.01$ versus the OGD/C+P group. Results are shown as mean ± SE of three independent experiments. The representative immunoblots are presented.

reduces neurologic infarction volumes, neurologic deficits, and apoptotic cell death in MCAO rats, which was demonstrated with concurrent use of NOX and PKC-δ inhibitors. In addition, we found that C+P also decreased ROS generation, NOX activity, NOX protein subunit expression, and the ratio of p-PKC-δ/PKC-δ, while increasing levels of MnSOD. NOX activity, NOX subunit protein expression, and ROS also decreased when subjected to NOX and PKC-δ inhibitors. Meanwhile, C+P therapy reduced ROS levels, NOX subunit protein expression, p-PKC-δ/PKC-δ, and increased MnSOD as well as suppressing PKC-δ membrane translocation and p47$^{\text{phox}}$ and PKC-δ interaction in the OGD/R model. Consistent with our previous research, PKC-δ and NOX seem to be key regulators by which C+P exerts its neuroprotective effects [5, 12]. This present study further explores the specific mechanism by which C+P inhibits oxidative stress and exerts neuroprotective effects through the PKC-δ/NOX/MnSOD pathway following ischemic stroke. This could be due to altered NOX subunit protein expression and PKC-δ regulation via phosphorylation, membrane translocation, and changes in the PKC-δ and p47$^{\text{phox}}$ interaction (Figure 8).

Using ischemic stroke models in a prior study, we found that administration of C+P enhanced neuroprotection by attenuating harmful metabolic cascades. These findings demonstrated C+P's cerebro-protective effects in models of ischemia, demonstrated through infarction volume reduc-

tions and decreased neurological deficits after stroke [5]. In addition, C+P's neuroprotective influence in ischemic stroke seems to be in part due to its ability to attenuate hyperglycolysis [9], disruption of the blood-brain barrier [22], inflammatory cascades [31], activation of inflammasomes [32], and apoptotic cell death [12]. C+P can induce therapeutic hypothermia; however, its neuroprotective ability post-stroke appears to be at least partially independent of its hypothermic effects [5, 9, 31, 32]. Recently, we reported that C+P suppressed neuroinflammatory reactions and NLRP3 inflammasome activation even without induction of hypothermia. We found that inhibition of the NLRP inflammasome could be achieved through reduced expression of several vital protein regulators, serving as possible focuses for neuroprotective therapy post-ischemic stroke [25]. In parallel, our current study indicates that C+P's neuroprotective effects after ischemic events are partially attributed to their hypothermic effects. However, C+P's cerebro-protective effects could also result from their effects on components of oxidative stress pathways, such as of PKC-δ, ROS, and NOX enzymes. Regardless of temperature control, treatment with C+P was also found to significantly reverse the post-MCAO decrease in MnSOD, a vital central nervous system antioxidant enzyme that strengthens cellular resistance to ROS after cerebral ischemia. Through these mechanisms, C+P therapy was found to significantly reduce infarction volumes, neurological deficits, and apoptotic cell
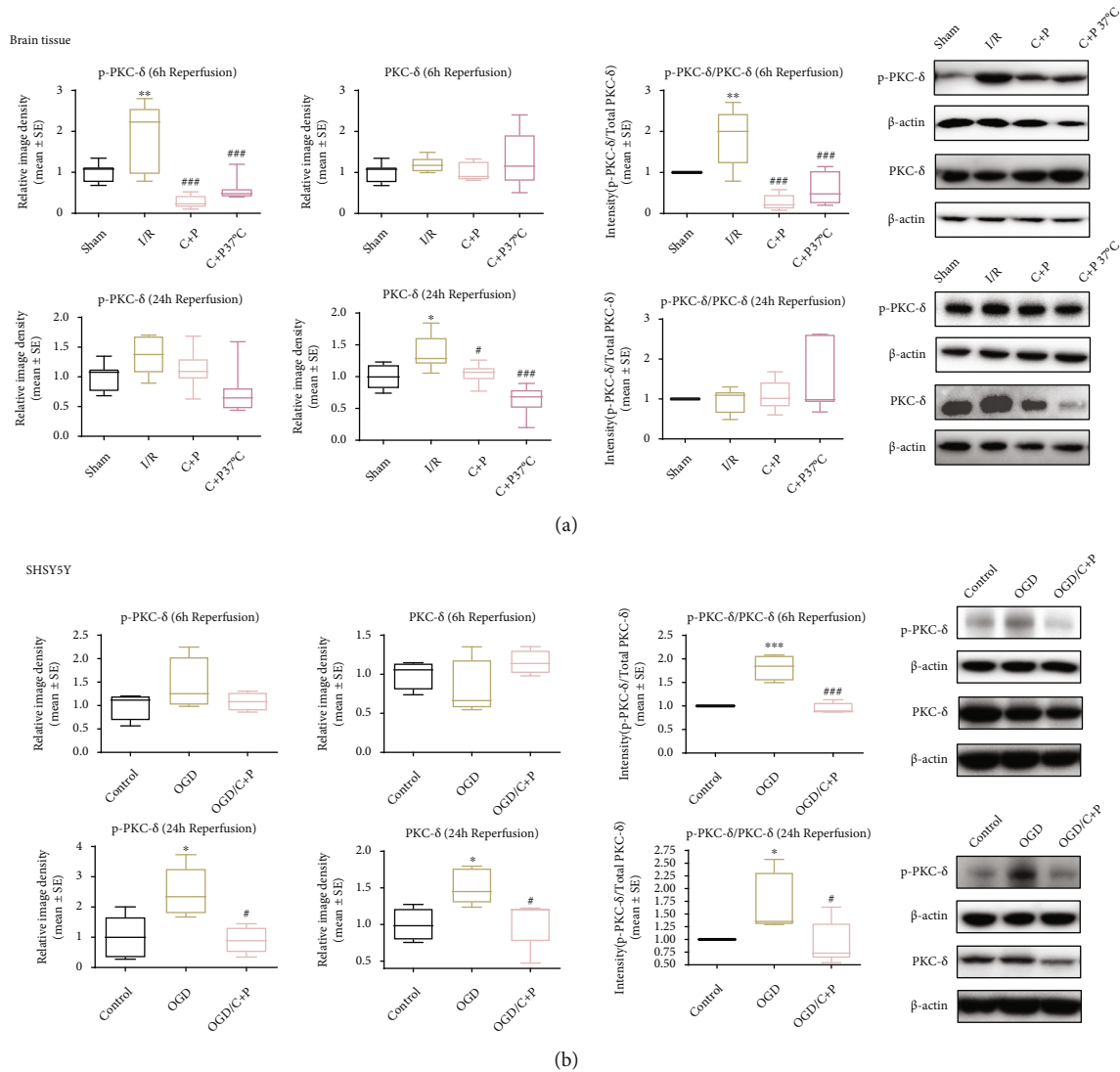
FIGURE 5: C+P decreased activation of PKC-δ induced by cerebral ischemia or OGD/R. (a) Representative bands of phosphorylated and total protein expressions of PKC-δ in brain tissue identified via Western blot at 6 and 24 hours of reperfusion. β-Actin served as an internal control. Bar graphs demonstrate semiquantitative levels of PKC-δ, identified using band density analysis. MCAO enhanced PKC-δ phosphorylation. C+P treatment reduced PKC-δ phosphorylation as compared with the stroke group at 6 hours of reperfusion. Total PKC-δ protein expression increased, but C+P reduced its level at 24 hours of reperfusion. Moreover, the ratio of p-PKC-δ/PKC-δ significantly increased post-MCAO but decreased with C+P treatment at 6 hours of reperfusion ($n = 7$). $^{*}p < 0.05$, $^{**}p < 0.01$ versus the sham group; $^{#}p < 0.05$, $^{###}p < 0.001$ versus the I/R group. Results are presented as mean ± SE. (b) Representative bands of both phosphorylated and total PKC-δ levels in SHSY5Y cells identified via Western blot at 6 and 24 hours of reoxygenation. β-Actin served as an internal control. Bar graphs display semiquantitative levels of PKC-δ as determined by band density analysis. The p-PKC-δ/PKC-δ ratio was significantly higher after OGD/R; however, it decreased after C+P administration at 6 hours of reoxygenation. Furthermore, both PKC-δ phosphorylation and the total levels of PKC-δ were significantly higher after OGD/R; however, C+P annulled this trend at 24 hours of reoxygenation. Similarly, OGD/R facilitated the raise in the p-PKC-δ/PKC-δ ratio, but C+P decreased this trend at 24 hours of reoxygenation. $^{*}p < 0.05$, $^{***}p < 0.001$ versus the OGD group; $^{#}p < 0.05$, $^{###}p < 0.001$ versus the OGD/C+P group. Results are shown as mean ± SE of three independent experiments.

death. C+P's neuroprotective effects seen in temperature-controlled environments reveal that their ability to enhance neuroprotection via pharmacological mechanisms is independent of hypothermia, which was confirmed by cell line experimentation.

ROS are vital components in a rising number of diseases, as they worsen oxidative stress while simultaneously enhancing tissue dysfunction [33]. Oxidative stress is a major factor

in neurologic damage resulting from ischemic stroke. Mitochondrial overproduction of ROS is theorized to be the driving force in oxidative stress. NOX enzymes, which transfer electrons across biological membranes, have been shown to be significant ROS generators in cerebral tissue postischemic event [34]. NOX enzymes use NADPH to catalyze molecular oxygen reduction, producing a superoxide anion. NADPH is supplied by the hexose monophosphate shunt for NOX
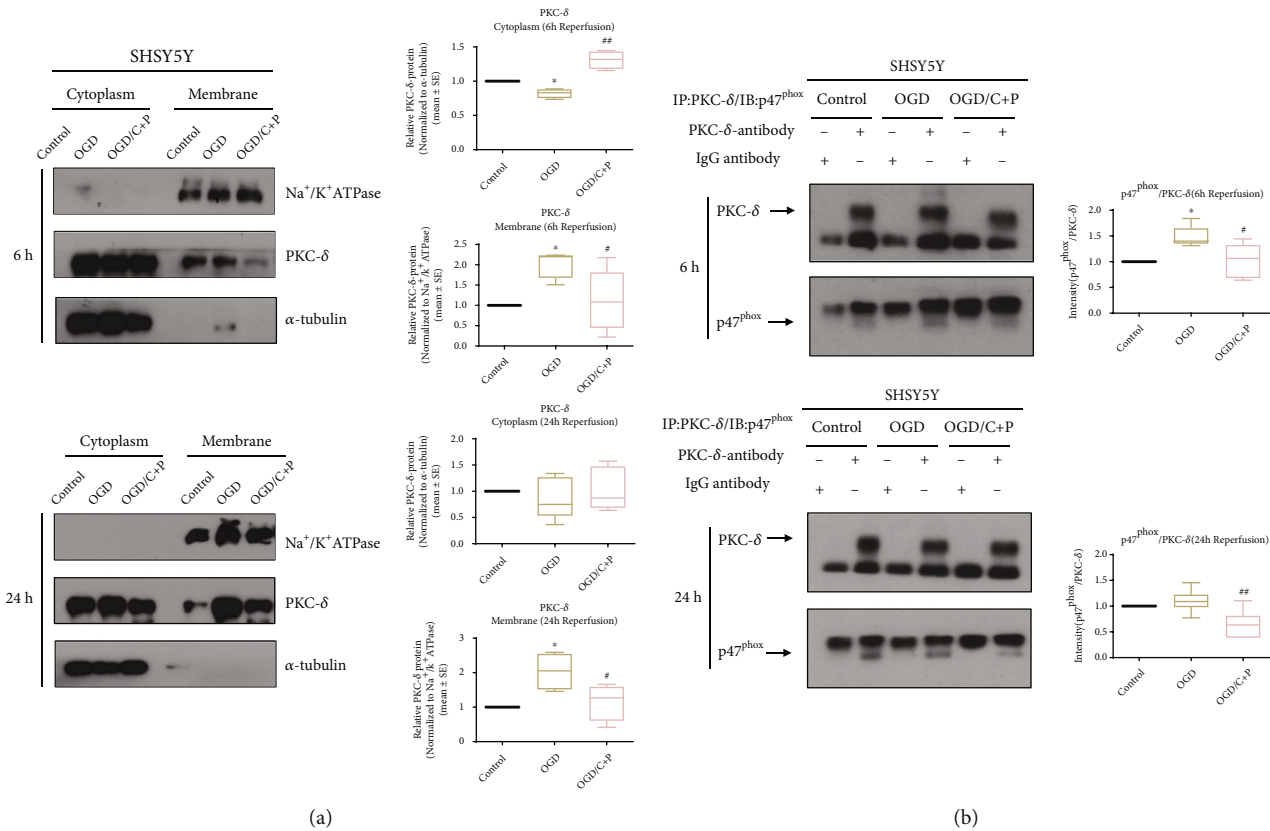
(a)   (b)

Figure 6: C+P suppressed the translocation of PKC-δ and interaction of PKC-δ with p47$^{\text{phox}}$ induced by OGD/R in SHSY5Y cells. (a) Representative bands of cytosolic and membrane PKC-δ identified using Western blot at 6 and 24 hours of reperfusion. Bar graphs show semiquantitative PKC-δ levels in the cytosol and membrane determined using band density analysis. Cytosolic PKC-δ expression decreased but increased in the membrane in the OGD/R group at 6 hours after reoxygenation as compared to the control group. Administration of C+P negated the changes of OGD/R-induced PKC-δ expression. No differences were detected in cytosolic PKC-δ expression in the OGD/R group at 24 hours of reoxygenation, but OGD/R increased membranous PKC-δ expression as compared to the control group. C+P attenuated the raised cellular membrane PKC-δ concentration. $^{*}p < 0.05$, as compared to the OGD group; $^{\#}p < 0.05$, $^{\#\#}p < 0.01$, as compared to the OGD/C+P group. All the quantifications were normalized to α-tubulin (cytosol) or Na^{+}/K^{+} ATPase (membrane), respectively. Results are shown as mean $\pm$ SE of three independent experiments. (b) Representative bands of coimmunoprecipitation of PKC-δ and p47$^{\text{phox}}$ in SHSY5Y cells, identified via the Western blot technique at 6 and 24 hours of reoxygenation. Bar graphs show the ratios of p47$^{\text{phox}}$/PKC-δ identified using band density analysis. IgG antibody served as the control. In comparison to IgG control, a significant enhancement in p47$^{\text{phox}}$ was detected in the immunoprecipitation complex with the PKC-δ antibody from cell lysates, which suggests a heightened interaction of PKC-δ and p47$^{\text{phox}}$. Moreover, the interaction of PKC-δ and p47$^{\text{phox}}$ increases after 6 hours of reoxygenation, while C+P treatment reduced the interaction. Although the interaction between the control and the OGD group was not significant at 24 hours of reoxygenation, the interaction did increase, and C+P treatment lowered the interaction between PKC-δ and p47$^{\text{phox}}$. $^{*}p < 0.05$ versus the OGD group; $^{\#}p < 0.05$, $^{\#\#}p < 0.01$ versus the OGD/C+P group. The data is represented as mean $\pm$ SE of three independent experiments.

enzymatic activity [35]. NOX metabolic activity worsens I/R injury [15], and inhibition of NOX has been shown to reduce neurologic damage after I/R injury [36]. The NOX complex includes both membrane-bound and cytosolic elements. In its resting state, the NOX catalytic region is composed of gp91$^{\text{phox}}$ and p22$^{\text{phox}}$, which are membrane-integrated flavocytochromes. The cytosolic elements include p47$^{\text{phox}}$ and p67$^{\text{phox}}$ [14, 37]. In order to activate NADPH oxidase, there must be membrane assembly of cytosolic p47$^{\text{phox}}$, p67$^{\text{phox}}$, p22$^{\text{phox}}$, and gp91$^{\text{phox}}$, resulting in activation of gp91$^{\text{phox}}$, the catalytic subunit [14]. It has been reported that I/R decreased p47$^{\text{phox}}$/p67$^{\text{phox}}$ in the cytosol and increased p47$^{\text{phox}}$/p67$^{\text{phox}}$/gp91$^{\text{phox}}$ in the membrane [38]. Upregulation of all major NOX subunits (p47$^{\text{phox}}$, p67$^{\text{phox}}$, p22$^{\text{phox}}$,

and gp91$^{\text{phox}}$) has also been found to be associated with increased NOX activity post-stroke [39–42]. Our current study showcased significantly decreased ROS levels, NOX enzyme activity, and levels of p47$^{\text{phox}}$, p67$^{\text{phox}}$, p22$^{\text{phox}}$, and gp91$^{\text{phox}}$ proteins after C+P therapy, consistent with the results of the NOX inhibitor group or PKC-δ inhibitor group. This furthers indicates a role for C+P in inhibition of oxidative stress through repression of the PKC-δ/NOX pathway.

PKC is a known component of upstream signaling in NADPH oxidase activation [38]. Further, chlorpromazine has been found to lower cadmium-induced oxidative renal damage, stemming from its ability to mitigate oxidative stress and stabilize calcium homeostasis via PKC inhibition [43]. Prior studies have shown that administration of C+P
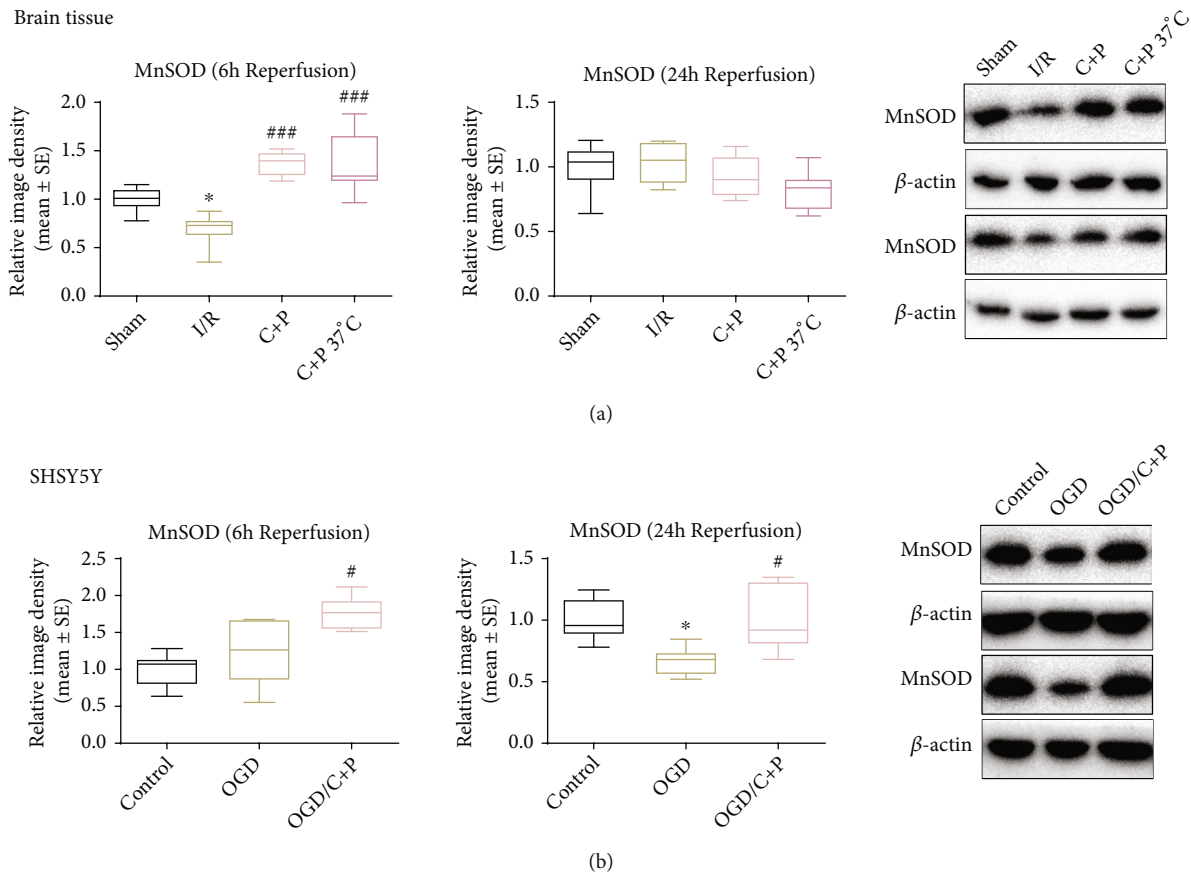
Brain tissue

(a)

(b)

Figure 7: C+P facilitated the expression of MnSOD after cerebral ischemia or OGD/R. (a) Representative bands of MnSOD in brain tissue as identified using Western blot at 6 and 24 hours of reperfusion. β-Actin served as an internal control. Semiquantitative levels of MnSOD are displayed in bar graphs, identified using band density analysis. MnSOD protein levels decreased after I/R. C+P administration significantly accelerated MnSOD expression at 6 hours of reperfusion ($n = 7$). $^*p < 0.05$ versus the sham group; $^{###}p < 0.001$ versus the I/R group. The data is presented as mean ± SE. (b) Representative bands of MnSOD expression in SHSY5Y cells as identified using Western blot at 6 and 24 hours of reoxygenation. β-Actin protein served as an internal control. Bar graphs show semiquantitative levels of MnSOD as identified using band density analysis. MnSOD protein levels decreased at 24 hours of reoxygenation. However, C+P therapy elevated MnSOD expression at 6 and 24 hours of reoxygenation. $^*p < 0.05$ versus the OGD group; $^#p < 0.05$ versus the OGD/C+P group. Results are shown as mean ± SE of three independent experiments.

reduces cell apoptosis via the NOX-Akt/PKC pathway [12]. PKC is a family of serine-threonine kinases, which control a wide variety of cell functions and have been involved in various diseases, including I/R injury [44–46]. This family is comprised of nine genes which express structurally related phospholipid-dependent kinases with separate regulatory mechanisms and distinct distribution among tissues. Various studies have connected PKC-δ to cell death in a variety of cultured cells [47], including neuronal cells [48]. PKC-δ-null mice have been shown to have a substantial reduction in stroke size (70%) when assessed against wild-type mice post transient MCAO and subsequent reperfusion therapy [46]. Additionally, NMDA-dependent upregulation of PKC-δ around the lesion significantly increased after I/R, along with other proteins known to be involved in neuronal death, like heat-shock proteins and haem oxygenase-1 [49–51]. PKC-δ appears to be a substantial part of oxidative stress regulation, likely through NOX stimulation in reperfusion injury [46]. In turn, PKC-δ activity is controlled by phosphorylation patterns and subcellular translocation in a

context-dependent manner [30]. For example, after stroke, the phosphorylation level of PKC-δ increases [52, 53]. This phosphorylated state activates PKC-δ, promoting NOX and ROS production [54]. Moreover, post-stroke, the translocation of PKC-δ from the cytosol to the membrane is facilitated, which impacts its function [38, 55]. PKC interactions with other proteins are also vital to the functions of PKC itself and the proteins it interacts with [56]. Prior research has demonstrated that ROS production is stimulated by activating the PKC-δ-p47^{phox} axis via PKC-δ activation, done by facilitating its translocation to the membrane and interacting with p47^{phox} in vascular smooth muscle cells [57]. In our current study, we observed that C+P inhibited ROS production ordinarily produced by the PKC-δ-p47^{phox} pathway. It accomplished this by reducing PKC-δ phosphorylation, PKC-δ membrane translocation, and PKC-δ and p47^{phox} interaction.

In mammalian cells, MnSOD is a crucial antioxidant enzyme located in the mitochondria. MnSOD detoxifies superoxide, the major byproduct of mitochondrial
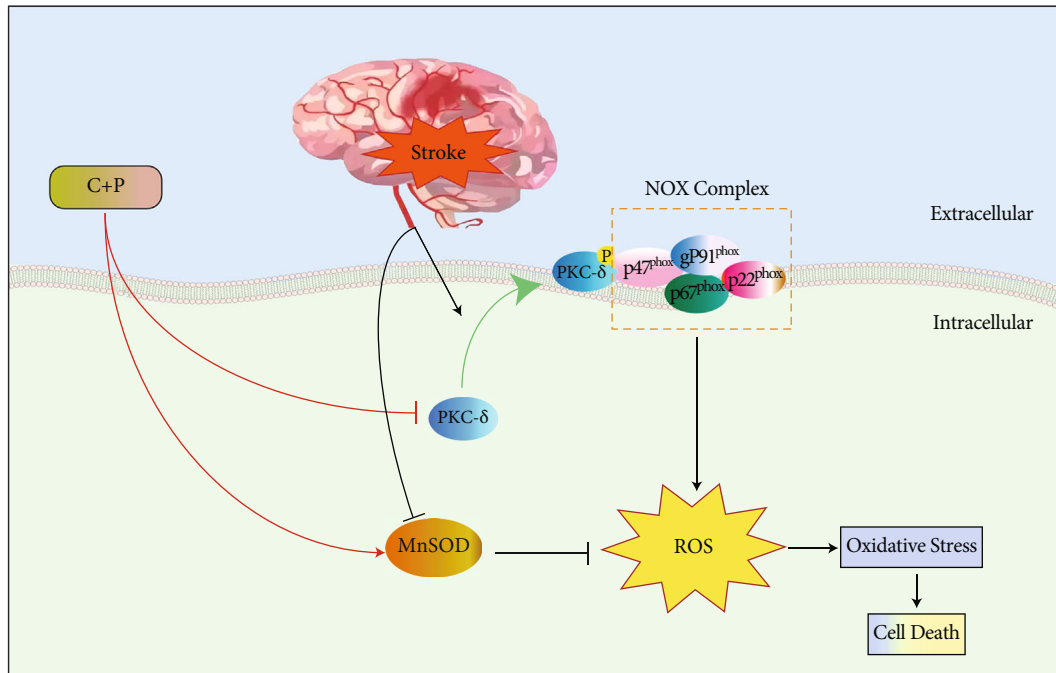
FIGURE 8: Schematic illustration of neuroprotection of C+P through the PKC-δ/NOX/MnSOD pathway. After I/R, PKC-δ translocated to the cell membrane is phosphorylated and activated. PKC-δ interacted with p47^{phox} which facilitates the activation of NOX. Moreover, MCAO also induced the elevated expression of NOX subunits gp91^{phox}, p47^{phox}, p67^{phox}, and p22^{phox}, resulting in NOX activation. NOX activation further increased ROS production and oxidative stress. Additionally, MnSOD expression is repressed after stroke. C+P suppressed both PKC-δ and NOX activation and promoted MnSOD expression, resulting in the reduced ROS production and oxidative stress.

respiration [58]. Consequently, MnSOD plays a crucial part in cell defense from oxidative stress [59]. MnSOD is highly expressed in neuronal cells and is imperative for maintaining protection from oxidative stress [60]. MnSOD is therefore a critical endogenous protective mechanism against cerebral ischemic damage. Protein expression of MnSOD was suppressed after reperfusion due to deactivation of the STAT3 gene, which regulates MnSOD expression in neuronal cells under regular conditions [61, 62]. OGD/R induction has also been found to downregulate MnSOD [63]. Moreover, MnSOD-deficient mice were found to have greater infarct volumes and levels of cell death post-ischemic event. Previous studies discerned that loss of MnSOD leads to reduced antioxidant activity and higher levels of uncoupled superoxide anion, which exacerbates ischemic injury and results in expansion of the infarcted penumbral area [64, 65]. Conversely, overexpression of MnSOD provided neuroprotection following cerebral I/R. For example, overexpressors of MnSOD had not increased brain hemorrhage and vascular endothelial cell death rates that were found in underexpressor and knockout models [66]. In our study, administration of C+P increased the expression of MnSOD, which may have further reduced the oxidative stress damage caused by ROS, conferring additional neuroprotection. These findings contribute not only to the growing section of literature exploring neuroprotective benefits of C+P therapy, but also to that of the antioxidant properties of MnSOD.

5. Conclusion

C+P dual therapy has evident neuroprotective benefits in the context of ischemic stroke. Several studies suggest that its benefits are conveyed through pharmacologically induced hypothermia. However, others have substantiated its benefits in temperature-controlled settings, thereby imploring the discovery of additional mechanisms for its neuroprotection. Our study sought to further explore these mechanisms and found that C+P-mediated antioxidant defense is through the PKC-δ/NOX/MnSOD pathway following acute ischemic stroke. The findings of this study provide valuable insight for future patients who suffer from strokes, as therapies targeting these pathways may significantly enhance neuroprotection. Future studies should focus on exploring these neuroprotective mechanisms in greater depth.

Data Availability

The data used to support the findings in this study are available from the corresponding author upon reasonable request.

Conflicts of Interest

The authors declare no conflict of interest.

Acknowledgments

References

[1] Y. Shimizu, A. Harashima, S. Munesue et al., "Neuroprotective effects of endogenous secretory receptor for advanced glycation end-products in brain ischemia," *Aging and Disease*, vol. 11, no. 3, pp. 547–558, 2020.

[2] G. B. Rajah and Y. Ding, "Experimental neuroprotection in ischemic stroke: a concise review," *Neurosurgical Focus*, vol. 42, no. 4, p. E2, 2017.

[3] Y. Ding, Y. Zhang, W. Zhang, J. Shang, Z. Xie, and C. Chen, "Effects of lipoic acid on ischemia-reperfusion injury," *Oxidative Medicine and Cellular Longevity*, vol. 2021, Article ID 5093216, 15 pages, 2021.

[4] M. Hollist, L. Morgan, R. Cabatbat, K. Au, M. F. Kirmani, and B. F. Kirmani, "Acute stroke management: overview and recent updates," *Aging and Disease*, vol. 12, no. 4, pp. 1000–1009, 2021.

[5] X. Geng, F. Li, J. Yip et al., "Neuroprotection by chlorpromazine and promethazine in severe transient and permanent ischemic stroke," *Molecular Neurobiology*, vol. 54, no. 10, pp. 8140–8150, 2017.

[6] A. M. Kuczynski, A. M. Demchuk, and M. A. Almekhlafi, "Therapeutic hypothermia: applications in adults with acute ischemic stroke," *Brain Circ*, vol. 5, no. 2, pp. 43–54, 2019.

[7] S. Liu, X. Geng, B. Forreider et al., "Enhanced beneficial effects of mild hypothermia by phenothiazine drugs in stroke therapy," *Neurological Research*, vol. 37, no. 5, pp. 454–460, 2015.

[8] B. Forreider, D. Pozivilko, Q. Kawaji, X. Geng, and Y. Ding, "Hibernation-like neuroprotection in stroke by attenuating brain metabolic dysfunction," *Progress in Neurobiology*, vol. 157, pp. 174–187, 2017.

[9] S. Guo, E. Cosky, F. Li et al., "An inhibitory and beneficial effect of chlorpromazine and promethazine (C + P) on hyperglycolysis through HIF-1α regulation in ischemic stroke," *Brain Research*, vol. 1763, article 147463, 2021.

[10] G. C. González-Muñoz, M. P. Arce, B. López et al., "Old phenothiazine and dibenzothiadiazepine derivatives for tomorrow's neuroprotective therapies against neurodegenerative diseases," *European Journal of Medicinal Chemistry*, vol. 45, no. 12, pp. 6152–6158, 2010.

[11] I. G. Stavrovskaya, M. V. Narayanan, W. Zhang et al., "Clinically approved heterocyclics act on a mitochondrial target and reduce stroke-induced pathology," *The Journal of Experimental Medicine*, vol. 200, no. 2, pp. 211–222, 2004.

[12] Y. Tong, K. B. Elkin, C. Peng et al., "Reduced apoptotic injury by phenothiazine in ischemic stroke through the NOX-Akt/PKC pathway," *Brain Sciences*, vol. 9, no. 12, p. 378, 2019.

[13] W. Li and S. Yang, "Targeting oxidative stress for the treatment of ischemic stroke: upstream and downstream therapeutic strategies," *Brain Circ*, vol. 2, no. 4, pp. 153–163, 2016.

[14] J. Shen, R. Rastogi, X. Geng, and Y. Ding, "Nicotinamide adenine dinucleotide phosphate oxidase activation and neuronal death after ischemic stroke," *Neural Regeneration Research*, vol. 14, no. 6, pp. 948–953, 2019.

[15] X. N. Tang, B. Cairns, J. Y. Kim, and M. A. Yenari, "NADPH oxidase in stroke and cerebrovascular disease," *Neurological Research*, vol. 34, no. 4, pp. 338–345, 2012.

[16] H. Yao, T. Ago, T. Kitazono, and T. Nabika, "NADPH oxidase-related pathophysiology in experimental models of stroke," *International Journal of Molecular Sciences*, vol. 18, no. 10, p. 2123, 2017.

[17] M. Li, L. Zhuan, T. Wang et al., "Apocynin improves erectile function in diabetic rats through regulation of NADPH oxidase expression," *The Journal of Sexual Medicine*, vol. 9, no. 12, pp. 3041–3050, 2012.

[18] T. Inoguchi, T. Sonta, H. Tsubouchi et al., "Protein kinase C-dependent increase in reactive oxygen species (ROS) production in vascular tissues of diabetes: role of vascular NAD (P) H oxidase," *J Am Soc Nephrol*, vol. 14, suppl 3, pp. S227–S232, 2003.

[19] H.-F. Huang, F. Guo, Y. Z. Cao, W. Shi, and Q. Xia, "Neuroprotection by manganese superoxide dismutase (MnSOD) mimics: antioxidant effect and oxidative stress regulation in acute experimental stroke," *CNS Neuroscience & Therapeutics*, vol. 18, no. 10, pp. 811–818, 2012.

[20] D. Wu, X. Zhi, Y. Duan et al., "Inflammatory cytokines are involved in dihydrocapsaicin (DHC) and regional cooling infusion (RCI)-induced neuroprotection in ischemic rat," *Brain Research*, vol. 1710, pp. 173–180, 2019.

[21] F. Wang, Y. Luo, F. Ling et al., "Comparison of neuroprotective effects in ischemic rats with different hypothermia procedures," *Neurological Research*, vol. 32, no. 4, pp. 378–383, 2010.

[22] F. Li, X. Geng, J. Yip, and Y. Ding, "Therapeutic target and cell-signal communication of chlorpromazine and promethazine in attenuating blood–brain barrier disruption after ischemic stroke," *Cell Transplantation*, vol. 28, no. 2, pp. 145–156, 2019.

[23] W. Wei, D. Wu, Y. Duan et al., "Neuroprotection by mesenchymal stem cell (MSC) administration is enhanced by local cooling infusion (LCI) in ischemia," *Brain Research*, vol. 1724, article 146406, 2019.

[24] Q. Jiang, X. Geng, J. Warren et al., "Hypoxia inducible factor-1α (HIF-1α) mediates NLRP3 inflammasome-dependent-pyroptotic and apoptotic cell death following ischemic stroke," *Neuroscience*, vol. 448, pp. 126–139, 2020.

[25] S. Guo, X. Geng, H. Lee, and Y. Ding, "Phenothiazine inhibits neuroinflammation and inflammasome activation independent of hypothermia after ischemic stroke," *Molecular Neurobiology*, vol. 58, no. 12, pp. 6136–6152, 2021.

[26] X. Geng, S. Parmar, X. Li et al., "Reduced apoptosis by combining normobaric oxygenation with ethanol in transient ischemic stroke," *Brain Research*, vol. 1531, pp. 17–24, 2013.

[27] R. Kochanski, C. Peng, T. Higashida et al., "Neuroprotection conferred by post-ischemia ethanol therapy in experimental stroke: an inhibitory effect on hyperglycolysis and NADPH oxidase activation," *Journal of Neurochemistry*, vol. 126, no. 1, pp. 113–121, 2013.

[28] X. Geng, P. Fu, X. Ji et al., "Synergetic neuroprotection of normobaric oxygenation and ethanol in ischemic stroke through improved oxidative mechanism," *Stroke*, vol. 44, no. 5, pp. 1418–1425, 2013.

[29] L. Roger, L. Jullien, V. Gire, and P. Roux, "Gain of oncogenic function of p 53 mutants regulates E-cadherin expression

uncoupled from cell invasion in colon cancer cells," *Journal of Cell Science*, vol. 123, pp. 1295–1305, 2010.

[30] Q. Yang, J. Langston, Y. Tang, M. Kiani, and L. Kilpatrick, "The role of tyrosine phosphorylation of protein kinase C delta in infection and inflammation," *International Journal of Molecular Sciences*, vol. 20, no. 6, p. 1498, 2019.

[31] L. Guan, S. Guo, J. Yip et al., "Artificial hibernation by phenothiazines: a potential neuroprotective therapy against cerebral inflammation in stroke," *Current Neurovascular Research*, vol. 16, no. 3, pp. 232–240, 2019.

[32] Q. Jiang, M. Wills, X. Geng, and Y. Ding, "Chlorpromazine and promethazine reduces brain injury through RIP1-RIP3 regulated activation of NLRP3 inflammasome following ischemic stroke," *Neurological Research*, vol. 43, no. 8, pp. 668–676, 2021.

[33] R. Rastogi, X. Geng, F. Li, and Y. Ding, "NOX activation by subunit interaction and underlying mechanisms in disease," *Frontiers in Cellular Neuroscience*, vol. 10, pp. 301–301, 2017.

[34] L. Zhang, J. Wu, X. Duan et al., "NADPH oxidase: a potential target for treatment of stroke," *Oxidative Medicine and Cellular Longevity*, vol. 2016, Article ID 5026984, 9 pages, 2016.

[35] S. W. Suh, B. S. Shin, H. Ma et al., "Glucose and NADPH oxidase drive neuronal superoxide formation in stroke," *Annals of Neurology*, vol. 64, no. 6, pp. 654–663, 2008.

[36] C. Hai, S. S. Yun, and P. H. Chan, "Inhibition of NADPH oxidase is neuroprotective after ischemia—reperfusion," *Journal of Cerebral Blood Flow and Metabolism*, vol. 29, no. 7, pp. 1262–1272, 2009.

[37] H. Sumimoto, K. Miyano, and R. Takeya, "Molecular composition and regulation of the Nox family NAD(P)H oxidases," *Biochemical and Biophysical Research Communications*, vol. 338, no. 1, pp. 677–686, 2005.

[38] H. Tang, C. S. Pan, X. W. Mao et al., "Role of NADPH oxidase in total salvianolic acid injection attenuating ischemia-reperfusion impaired cerebral microcirculation and neurons: implication of AMPK/Akt/PKC," *Microcirculation*, vol. 21, no. 7, pp. 615–627, 2014.

[39] Y. Luo, H. Chen, B. Tsoi, Q. Wang, and J. Shen, "Danggui-Shaoyao-San (DSS) ameliorates cerebral ischemia-reperfusion injury via activating SIRT1 signaling and inhibiting NADPH oxidases," *Frontiers in Pharmacology*, vol. 12, article 653795, 2021.

[40] I. Kusaka, G. Kusaka, C. Zhou et al., "Role of AT1 receptors and NAD(P)H oxidase in diabetes-aggravated ischemic brain injury," *American Journal of Physiology. Heart and Circulatory Physiology*, vol. 286, no. 6, pp. H2442–H2451, 2004.

[41] Q. Jin, Y. Jiang, L. Fu, Y. Zheng, Y. Ding, and Q. Liu, "Wenxin granule ameliorates hypoxia/reoxygenation-induced oxidative stress in mitochondria via the PKC-δ/NOX2/ROS pathway in H9c2 cells," *Oxidative Medicine and Cellular Longevity*, vol. 2020, Article ID 3245483, 16 pages, 2020.

[42] Q. Lu, M. S. Wainwright, V. A. Harris et al., "Increased NADPH oxidase-derived superoxide is involved in the neuronal cell death induced by hypoxia-ischemia in neonatal hippocampal slice cultures," *Free Radical Biology & Medicine*, vol. 53, no. 5, pp. 1139–1151, 2012.

[43] B. Xu, Z. F. Xu, Y. Deng, and J. H. Yang, "Protective effects of chlorpromazine and verapamil against cadmium-induced kidney damage in vivo," *Experimental and Toxicologic Pathology*, vol. 62, no. 1, pp. 27–34, 2010.

[44] M. F. Olive and R. O. Messing, "Protein kinase C isozymes and addiction," *Molecular Neurobiology*, vol. 29, no. 2, pp. 139–154, 2004.

[45] P. J. Parker and J. Murray-Rust, "PKC at a glance," *Journal of Cell Science*, vol. 117, no. 2, pp. 131-132, 2004.

[46] W. H. Chou and R. O. Messing, "Protein kinase C isozymes in stroke," *Trends in Cardiovascular Medicine*, vol. 15, no. 2, pp. 47–51, 2005.

[47] C. Brodie and P. M. Blumberg, "Regulation of cell apoptosis by protein kinase c delta," *Apoptosis*, vol. 8, no. 1, pp. 19–27, 2003.

[48] V. Anantharam, M. Kitazawa, J. Wagner, S. Kaul, and A. G. Kanthasamy, "Caspase-3-dependent proteolytic cleavage of protein kinase Cdelta is essential for oxidative stress-mediated dopaminergic cell death after exposure to methylcyclopentadienyl manganese tricarbonyl," *The Journal of Neuroscience*, vol. 22, no. 5, pp. 1738–1751, 2002.

[49] S. Miettinen, R. Roivainen, R. Keinänen, T. Hökfelt, and J. Koistinaho, "Specific induction of protein kinase C delta subspecies after transient middle cerebral artery occlusion in the rat brain: inhibition by MK-801," *The Journal of Neuroscience*, vol. 16, no. 19, pp. 6236–6245, 1996.

[50] F. A. Welsh, D. J. Moyer, and V. A. Harris, "Regional expression of heat shock protein-70 mRNA and c-fos mRNA following focal ischemia in rat brain," *Journal of Cerebral Blood Flow and Metabolism*, vol. 12, no. 2, pp. 204–212, 1992.

[51] J. Koistinaho, S. Miettinen, R. Keinänen, N. Vartiainen, R. Roivainen, and J. T. Laitinen, "Long-term induction of haem oxygenase-1 (HSP-32) in astrocytes and microglia following transient focal brain ischaemia in the rat," *The European Journal of Neuroscience*, vol. 8, no. 11, pp. 2265–2272, 1996.

[52] J. Wang, X. Fu, D. Zhang et al., "ChAT-positive neurons participate in subventricular zone neurogenesis after middle cerebral artery occlusion in mice," *Behavioural Brain Research*, vol. 316, pp. 145–151, 2017.

[53] B. Zhao, J. Wang, L. Liu et al., "Annexin A1 translocates to nucleus and promotes the expression of pro-inflammatory cytokines in a PKC-dependent manner after OGD/R," *Scientific Reports*, vol. 6, no. 1, p. 27028, 2016.

[54] C. M. Yang, S. H. Yang, T. H. Lee et al., "Evaluation of anti-inflammatory effects of Helminthostachys zeylanica extracts via inhibiting bradykinin-induced MMP-9 expression in brain astrocytes," *Molecular Neurobiology*, vol. 53, no. 9, pp. 5995–6005, 2016.

[55] T. Shimohata, H. Zhao, J. H. Sung, G. Sun, D. Mochly-Rosen, and G. K. Steinberg, "Suppression of deltaPKC activation after focal cerebral ischemia contributes to the protective effect of hypothermia," *Journal of Cerebral Blood Flow and Metabolism*, vol. 27, no. 8, pp. 1463–1475, 2007.

[56] S. Somara and K. N. Bitar, "Direct association of calponin with specific domains of PKC-alpha," *American Journal of Physiology. Gastrointestinal and Liver Physiology*, vol. 295, no. 6, pp. G1246–G1254, 2008.

[57] P. Lv, S. B. Miao, Y. N. Shu et al., "Phosphorylation of smooth muscle 22α facilitates angiotensin II-induced ROS production via activation of the PKCδ-P47phox axis through release of PKCδ and actin dynamics and is associated with hypertrophy and hyperplasia of vascular smooth muscle cells in vitro and in vivo," *Circulation Research*, vol. 111, no. 6, pp. 697–707, 2012.

[58] D. Candas and J. J. Li, "MnSOD in oxidative stress response-potential regulation via mitochondrial protein influx," *Antioxidants & Redox Signaling*, vol. 20, no. 10, pp. 1599–1617, 2014.

[59] P. H. Chan, "Role of oxidants in ischemic brain damage," *Stroke*, vol. 27, no. 6, pp. 1124–1129, 1996.

[60] G. W. Kim, T. Kondo, N. Noshita, and P. H. Chan, "Manganese superoxide dismutase deficiency exacerbates cerebral infarction after focal cerebral ischemia/reperfusion in mice: implications for the production and role of superoxide radicals," *Stroke*, vol. 33, no. 3, pp. 809–815, 2002.

[61] M. Cai, Y. Ma, W. Zhang et al., "Apigenin-7-O-β-D-(-6'-p-coumaroyl)-glucopyranoside treatment elicits neuroprotective effect against experimental ischemic stroke," *International Journal of Biological Sciences*, vol. 12, no. 1, pp. 42–52, 2016.

[62] J. E. Jung, G. S. Kim, P. Narasimhan, Y. S. Song, and P. H. Chan, "Regulation of Mn-superoxide dismutase activity and neuroprotection by STAT3 in mice after cerebral ischemia," *The Journal of Neuroscience*, vol. 29, no. 21, pp. 7003–7014, 2009.

[63] W. Xie, T. Zhu, P. Zhou et al., "Notoginseng leaf triterpenes ameliorates OGD/R-induced neuronal injury via SIRT1/2/3-Foxo3a-MnSOD/PGC-1α signaling pathways mediated by the NAMPT-NAD pathway," *Oxidative Medicine and Cellular Longevity*, vol. 2020, Article ID 7308386, 15 pages, 2020.

[64] K. Murakami, T. Kondo, M. Kawase et al., "Mitochondrial susceptibility to oxidative stress exacerbates cerebral infarction that follows permanent focal cerebral ischemia in mutant mice with manganese superoxide dismutase deficiency," *The Journal of Neuroscience*, vol. 18, no. 1, pp. 205–213, 1998.

[65] M. Fujimura, Y. Morita-Fujimura, M. Kawase et al., "Manganese superoxide dismutase mediates the early release of mitochondrial cytochrome C and subsequent DNA fragmentation after permanent focal cerebral ischemia in mice," *The Journal of Neuroscience*, vol. 19, no. 9, pp. 3414–3422, 1999.

[66] C. M. Maier, L. Hsieh, T. Crandall, P. Narasimhan, and P. H. Chan, "Evaluating therapeutic targets for reperfusion-related brain hemorrhage," *Annals of Neurology*, vol. 59, no. 6, pp. 929–938, 2006.